Desalination and Water Treatment
www.deswater.com

doi: 10.5004/dwt.2017.20725

75 (2017) 115–123
May

Removal of arsenic(III) ions from aqueous solutions by modified hazelnut shell

Seda Sert[a,*], Ali Çelik[b], Vedia Nüket Tirtom[b]

[a] *Applied Science Research Center, Celal Bayar University, 45140, Muradiye-Manisa, Turkey, Tel. +902362013152; Fax: +902362012607; email: seda.yetim@cbu.edu.tr*
[b] *Department of Chemistry, Faculty of Science and Arts, Celal Bayar University, 45140, Muradiye-Manisa, Turkey, Tel. +902362013152, +902362013172; emails: ali.celik@bayar.edu.tr (A. Çelik), nuket.tirtom@bayar.edu.tr (V.N. Tirtom)*

Received 10 August 2016; Accepted 21 March 2017

ABSTRACT

In this study, modified hazelnut shells (HS) were used to remove As(III) ions from aqueous solutions. For this purpose, $FeCl_3$ and $FeCl_3$ + NaOH were used as modifying agents. Several important parameters influencing the adsorption of As(III) ions such as contact time, pH, temperature and initial metal concentration were investigated following batch experiments. From the results, it is indicated that temperature 20°C and solution pH = 9.0 are the optimum conditions for adsorption. Maximum adsorption experimental capacities of HS that was treated with $FeCl_3$ and $FeCl_3$ + NaOH were 4.37 and 11.84 mg g^{-1} for arsenic, respectively. The adsorption data at optimum conditions were analyzed by Freundlich, Langmuir, Dubinin–Radushkevich and Temkin isotherm models, and it was found that Freundlich isotherm model gives better fit. Thermodynamic parameters such as enthalpy change ($\Delta H°$), entropy change ($\Delta S°$) and free energy change ($\Delta G°$) were also calculated. These results were indicated that the adsorption of arsenic on HS is exothermic and proceeds spontaneously. Additionally, it can be said that these adsorptions are physical because the Gibbs free energy change ($\Delta G°$) for both adsorbents were found lower than 20 kJ mol^{-1}.

Keywords: Adsorption; Arsenic; Hazelnut shell; Natural adsorbents

1. Introduction

Arsenic is a ubiquitous element in earth's crust and naturally present in soil and water [1–3]. Weathering of rock is the major natural source of inorganic arsenic, and it is also released by human activities such as mining, discharges from coal fired, petroleum refining, etc. [4,5]. The presence of arsenic in groundwater is mostly due to minerals dissolving naturally from rocks and soils [6].

Inorganic and organic arsenic occur naturally in the environment, with inorganic forms being most abundant [7]. Inorganic arsenic is found in two prevalent oxidation states at environmentally relevant pH, arsenite (As(III)) and arsenate (As(V)) [8]. Main species of arsenite are H_3AsO_3, $H_2AsO_3^-$, $HAsO_3^{2-}$ and AsO_3^{3-} [9]. The uncharged H_3AsO_3 dominates at pH lower than 9.0 under reducing conditions in groundwater with low oxygen levels [7,9]. Arsenite is the more mobile, more toxic and more difficult to remove species due to its uncharged form at most pH [8].

Arsenic is potentially toxic to humans as chronic effects for a long time intake food and drinking water with arsenic contamination [10]. Drinking of arsenic contaminated water for long periods of time causes lung, bladder, kidney, liver and non-melanoma skin cancers [11–13]. It also causes changes in pigmentation of skin (arsenicosis), skin thickening (hyperkeratosis), neurological disorders, muscular weakness, loss of appetite and nausea [5]. In the coming years the arsenic groundwater consumption is estimated to directly cause over 6,500 deaths a year, and over 2.5 million people may develop arsenicosis in the next 50 years [14].

To abate health problems associated with arsenic in drinking water, the World Health Organization (WHO), European Commission (EC) and United States Environmental Protection Agency (USEPA) reduced the maximum contaminant level of

---

* Corresponding author.

1944-3994/1944-3986

arsenic in drinking water from 50 to 10 μg L^{-1} [15]. Therefore, developing economical, effective and reliable treatment techniques for arsenic removal from groundwater is critical and has gained considerable attention in recent years [9].

In order to keep arsenic limit below 10 μg L^{-1}, several methods have been developed, including coagulation and flocculation, precipitation, adsorption, ion exchange and membrane filtration [16]. Most of the established technologies for arsenic removal use the several of these processes, either at the same time or in sequence [17]. These well-established approaches have their respective advantages and certain inherent limitations that include the generation of toxic waste, low arsenic removal efficiency and high cost [18]. Adsorption systems use the affinity of different materials to remove soluble pollutants from an aqueous phase to the surface of a solid phase. Advantages of adsorption processes over other techniques are: its low running cost, the absence of electrical supply and its low maintenance requirements [14].

So far, various adsorbents for arsenic removal have been developed that include such natural materials as orange juice residue [19], coconut coir pith [20], waste rice husk [21], eggshell [22], biomass [23], chestnut shell [24], etc. Natural adsorbents have several advantages such as low cost, non-toxicity, biocompatibility, biodegradability and environment friendly. Besides it has been proved that arsenic has affinity toward iron compounds. Thus, many researchers have tested arsenic removal using iron-containing materials as adsorbent. For example, attempts have been made using iron oxide coated sand [25], alumina iron hydroxide coated [26], iron oxide loaded slag [27], iron(III) loaded resin [28], iron-impregnated chitosan [7], Kula ebonite and zeolite treated with iron(III) chloride [29] to remove arsenic from aqueous system.

In the present study, we investigated the adsorption behavior of inorganic As(III) ions by hazelnut shell (HS) modified with $FeCl_3$ and $FeCl_3$ + NaOH. A series of batch experiments were conducted to investigate the adsorption characteristics of As(III) ions onto these adsorbents. Scanning electron microscopy (SEM) was used for the observation of the surface morphology and structural analysis on both adsorbents before and after the arsenic adsorption.

2. Materials and methods

2.1. Reagents

All the chemicals were of analytical grade. $FeCl_3$, NaOH, HCl, CH_3COOH, $NaCH_3COO.3H_2O$, KH_2PO_4, $KHPO_4$ and NH_3 were purchased from Merck (Darmstadt, Germany). As_2O_3 was purchased from Sigma-Aldrich (Seelze, Germany). Hazelnuts were originated from Adapazari, Turkey. Ultrapure deionized water used in all the study was purified by Millipore ultrapure water purification system.

2.2. Instruments

Arsenic concentration measurements were carried out using Varian 220 FS atomic absorption spectrometry (AAS) and Varian VGA 77 continuous flow hydride generation (HG) system. The pH of solution was measured with a Hanna P211 microprocessor pH-meter using a combined glass electrode. The shaking experiments were carried out in a water bath with shaker Memmert, and drying was carried out in a Nuve EN 400 drying oven.

2.3. Preparation of adsorbents

Hazelnuts are broken, and the shells are separated. They were sieved with a grinded mill to obtain 149 μm particle size and washed with distilled water to remove the soluble compounds then dried. Two different modifications were applied to the washed adsorbent.

- Modification with $FeCl_3$: 10 g of dry adsorbent was transferred into a beaker containing 50.0 mL of 0.5 M $FeCl_3$ solutions, and the suspensions were stirred with magnetic stirrer for 12 h.
- Modification with $FeCl_3$ + NaOH: 10 g of dry adsorbent was transferred into a beaker containing 25.0 mL of 0.5 M $FeCl_3$ + 25.0 mL 0.2 M NaOH solutions, and the suspensions were stirred with magnetic stirrer for 12 h.

The treated adsorbents were separated from the solution by decantation and washed with distilled water to remove the soluble compounds. They were then dried at 60°C in an oven and used in the adsorption studies.

2.4. Preparation of solutions

1,000 mg L^{-1} stock As(III) solution was prepared by dissolving 0.3301 ± 0.0002 g As_2O_3 in 10% NaOH. The solution was acidified by adding concentrated HCl and diluted to 250 mL with ultrapure deionized water. As_2O_3 does not dissolve completely in water; therefore, As_2O_3 should be dissolved in NaOH, and the basic solution could be neutralized by an acid solution, such as HCl. Stock solution was diluted stepwise (100, 10, 1 and 0.1 mg L^{-1}) to prepare the intermediate stock solution. Standard solutions of arsenic (2, 4, 6, 8, 10 and 12 μg L^{-1}) were prepared by dilution of appropriate volume of 0.1 mg L^{-1} As(III) solution. pH experiments were carried out in buffer solution, and they were prepared by using conjugated acid/base couples of $CH_3COOH/NaCH_3COO.3H_2O$ for pH = 4.0, KH_2PO_4/K_2HPO_4 for pH = 7.0 and NH_4^+/NH_3 for pH = 9.0.

2.5. Adsorption

Adsorption experiments were carried out by batch technique. 0.10 ± 0.02 g of each adsorbent (HS modified with $FeCl_3$ and $FeCl_3$ + NaOH) was put in a beaker containing 25 mL of 50 μg L^{-1} As(III) solutions. The shaking was carried out in a thermostated water bath with shaker under constant stirring at 140 rpm. After decantation, the concentration of As(III) was analyzed by HG-AAS at 193.7 nm by acetylene/air flame method. All the experiments were carried out 3 times. The percentage adsorption of arsenic on adsorbate from aqueous solution was calculated as follows (Eq. 1):

$$(\%A) = \frac{C_{\text{int}} - C_{\text{fin}}}{C_{\text{int}}} \times 100 \quad (1)$$

where C_{int} and C_{fin} are the initial and final arsenic concentrations in the solution, respectively. Parameters affecting the adsorption performance like contact time (0.5, 1, 2, 4, 6, 8, 12 and 24 h), pH (4, 7 and 9), temperature (20°C, 30°C and 40°C) and initial arsenic concentration (0.05, 0.20, 1.00, 2.50, 5.00, 10.00, 25.00, 50.00, 75.00, 100.00 and 125.00 mg L^{-1}) were experimented sequentially. But the adsorbent used was kept as constant at 0.10 ± 0.02 g in all experiments. The amount of As(III) ion adsorbed was calculated according to the following equation (Eq. 2):

$$q_e = \frac{(C_{\text{int}} - C_{\text{fin}}) \times V}{m} \tag{2}$$

where q_e (mg g^{-1}) is the amount of As(III) ions adsorbed by HS modified with $FeCl_3$ and $FeCl_3$ + NaOH; V (L) is the volume of the solution; and m (g) is the mass of adsorbent used.

2.6. Characterization of HS modified with $FeCl_3$ and $FeCl_3$ + NaOH

Surface morphology of adsorbents was determined by SEM (XL30-SFEG, FEI/Philips). Surface characterization was carried out on bare HS, HS modified with $FeCl_3$ and $FeCl_3$ + NaOH and also each modified HS treated with As(III) solutions. Chemical compositions of bare and modified adsorbents treated with As(III) were analyzed with energy-dispersive x-ray (EDX) detector. Percentage of some structural elements (C, N, O and S), iron and arsenic were determined. Elemental analysis results give an idea about how much iron linked on HS during modification and how much arsenic was removed by adsorbents.

The Brunauer–Emmett–Teller (BET) surface areas of modified HSs were calculated from N_2 adsorption by using the BET method with Micromeritics model, Flowsorb II-2300 adsorption meter.

The materials have been characterized by fourier transform infrared spectroscopy (FTIR) spectrometry using Agilent Cary 660 with incorporation of attenuated total reflectance (ATR) accessory. Analytical conditions correspond to the collection of four scans with a resolution of 4 cm^{-1}.

X-ray diffractometer (XRD) analysis of powder samples was performed using an XRD PANalytical Empyrean (1D pixel detector) using the Cu Kα radiation.

3. Results and discussion

3.1. Effect of contact time

Fig. 1 also shows the time profiles of As(III) adsorption on HS modified with $FeCl_3$ and $FeCl_3$ + NaOH. It can be observed that the adsorption capacities initially increased along with contact time and then decreased, and finally reach equilibrium in 24 h. Adsorption of As(III) ions showed an increasing trend up to a reaction time of 4 and 2 h on HS modified with $FeCl_3$ and HS modified with $FeCl_3$ + NaOH, respectively, than the adsorption percentage decreases for both adsorbent. The reason for this decrease is thought to be due to desorption. Maximum adsorption was determined at 4 and 2 h for HS modified with $FeCl_3$ and HS modified with $FeCl_3$ + NaOH, and optimum adsorption time was chosen as 4 and 2 h, respectively.

3.2. Effect of pH

The effect of pH on As(III) adsorption was studied in pH of 4.0 ± 0.3, 7.0 ± 0.2 and 9.0 ± 0.2. The experiments were carried out with HS modified with $FeCl_3$ and $FeCl_3$ + NaOH at 4 and 2 h, respectively. The effect of the pH on adsorption capacity is shown in Fig. 2.

In order to understand the pH effect, it is necessary to examine the charge of both bare HS and modified active groups. Unmodified ionic groups of HS are predominant in charge of the adsorbent (point of zero charge [PZC] = 4.0 and 4.2). But active group for adsorption is iron oxyhydroxide. At Kosmulski's review [30] indicated that PZC of some iron oxyhydroxide minerals like goethite are 9.0 and above.

In the light of this information:

- At pH 4.0 as shown in the arsenic speciation diagram (Fig. 3), As(III) is predominately present in the form of

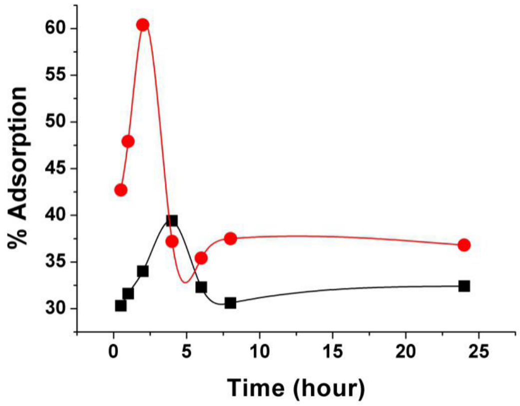

Fig. 1. Effect of contact time on removal of As(III) by modified hazelnut shell: temperature – 25°C; initial concentration – 0.05 mg L^{-1} and 0.1 g adsorbent (■: HS modified with $FeCl_3$; ●: HS modified with $FeCl_3$ + NaOH).

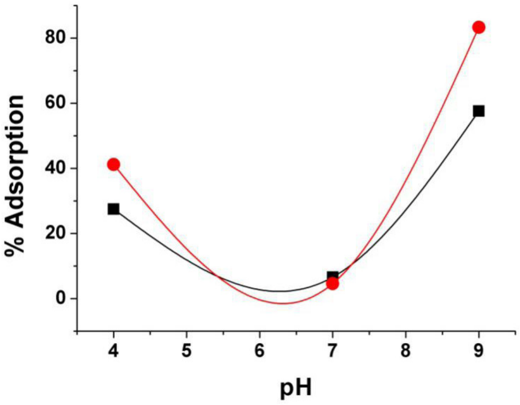

Fig. 2. Effect of pH on removal of As(III) by modified hazelnut shell: contact time for HS modified with $FeCl_3$ and HS modified with $FeCl_3$ + NaOH – 4 and 2 h, respectively; optimum temperature – 25°C, initial concentration – 0.05 mg L^{-1} and 0.1 g adsorbent (■: HS modified with $FeCl_3$; ●: HS modified with $FeCl_3$ + NaOH).

H_3AsO_3, and positive groups of HS and iron oxyhydroxide groups adsorp the neutral arsenic species.

- At pH = 7.0 adsorbent is negative excluding positively charged iron oxyhydroxide groups, and arsenic species are also neutral but no adsorption occurred. Competitive phosphate ions existing in buffer solution could be effective, or negative charge of sorbents could keep arsenic away from the surface.
- At pH = 9.0 some of H_3AsO_3 converts to $H_2AsO_3^-$, and positively charged iron oxyhydroxide groups adsorp arsenic effectively.

The maximum adsorption of As(III) ions on both adsorbents occurred at pH = 9.0; therefore, this pH value was selected as the optimum pH throughout the study.

3.3. Thermodynamics of adsorption

Temperature effects on adsorption are shown in Fig. 4. As shown in Fig. 4, adsorption was decreased with temperature for both adsorbents. Maximum adsorption was observed at 20°C. Temperature-dependent distribution coefficient for adsorption of arsenic was computed as follows:

$$K_d = \frac{C_{\text{int}} - C_e}{C_e} \tag{3}$$

where C_{int} and C_e are the initial and equilibrium arsenic concentrations (mg L^{-1}), respectively.

Thermodynamic parameters such as free energy change ($\Delta G°$), enthalpy change ($\Delta H°$) and entropy change ($\Delta S°$) were determined using the following equations:

$$\Delta G° = -RT \ln K_d \tag{4}$$

$$\Delta G° = \Delta H° - T\Delta S° \tag{5}$$

These equations are combined to obtain van't Hoff equation:

$$\ln K_d = \frac{-\Delta H°}{T.R} + \frac{\Delta S°}{R} \tag{6}$$

where $\Delta G°$ is standard Gibbs free energy change (J mol^{-1}); R is universal gas constant (8.314 J mol^{-1} K^{-1}); and T is absolute temperature (K). The change of enthalpy ($\Delta H°$) and entropy ($\Delta S°$) can be obtained from the y-axis intercept and slope of van't Hoff plot presented in Fig. 5. Values of the standard Gibbs free energy change for the adsorption process were obtained from Eq. (5), and all of thermodynamic parameters were listed in Table 1. The negative values of $\Delta H°$ indicated that the adsorption process was exothermic in nature. The negative values of $\Delta G°$ shows an adsorption process proceeds spontaneously.

3.4. Adsorption isotherms

The adsorbents were mixed by varying the initial concentrations (0.05, 0.20, 1.00, 2.50, 5.00, 10.00, 25.00, 50.00, 75.00,

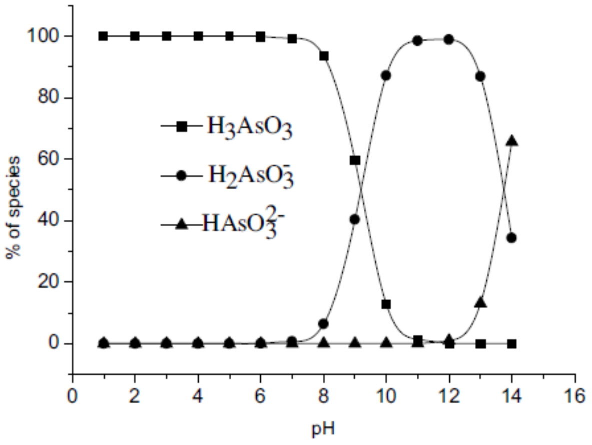

Fig. 3. Speciation diagram of As(III) ions.

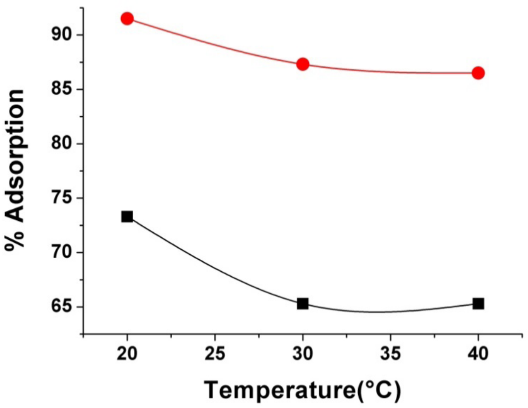

Fig. 4. Effect of temperature on removal of As(III) by modified hazelnut shell: contact time for HS modified with $FeCl_3$ and HS modified with $FeCl_3$ + NaOH – 4 and 2 h, respectively; optimum pH – 9.0 ± 0.2; initial concentration – 0.05 mg L^{-1} and 0.1 g adsorbent (■: HS modified with $FeCl_3$; ●: HS modified with $FeCl_3$ + NaOH).

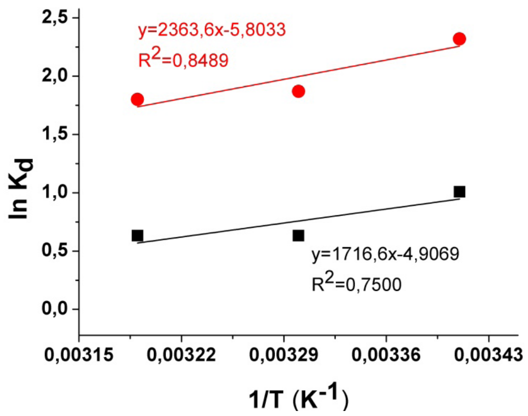

Fig. 5. Plot of $\ln K_d$ vs. $1/T$ (■: HS modified with $FeCl_3$; ●: HS modified with $FeCl_3$ + NaOH).

100.00 and 125.00 mg L^{-1}) at pH = 9.0 and 20°C. Fig. 6 shows the plots of q_e vs. equilibrium concentration of As(III) on the both adsorbents.

The analysis of the isotherms data by fitting them into different isotherm models is an important step to find the suitable model that can be used for design process. The linear form of Langmuir isotherm is given as follows:

$$\frac{1}{q_e} = \frac{1}{b.q_m} \cdot \frac{1}{c_e} + \frac{1}{q_m} \tag{7}$$

where q_e is the equilibrium adsorption capacity of adsorbent in mg As(III) per g of adsorbent; C_e is the equilibrium concentration of As(III) ions in mg L^{-1}; q_m is the maximum amount of As(III) adsorbed in mg As(III) per g of adsorbent; and b is the constant that refers to the bonding energy of adsorption in L mg^{-1}.

The linear form of Freundlich isotherm is given as:

$$\log q_e = \log K_f + \frac{1}{n} \log C_e \tag{8}$$

where K_f (mg g^{-1}) is a constant related to the adsorption affinity, and $1/n$ is related to heterogeneity of the adsorption sites.

The linear form of Dubinin–Radushkevich isotherm is given as follows:

$$\ln q_e = \ln q_m - k\varepsilon^2 \tag{9}$$

where q_e and q_m have the same meaning as before; k (mol^2 J^{-2}) is a constant related to the adsorption energy; and ε is the Polanyi potential given by Eq. (10):

$$\varepsilon = RT \ln\left(1 + \frac{1}{C_e}\right) \tag{10}$$

The linear form of Temkin isotherm is given as:

$$q_e = B \ \ln A \ + \ B \ \ln \ C_e \tag{11}$$

where $B = RT/b_T$ is a parameter connected to the heat of adsorption. A indicates maximum binding energy (L g^{-1}); b_T indicates Temkin constant associated to heat of adsorption (J mg^{-1}). Constants of isotherm models and the linear regression correlation (R^2) are given in Table 2. Comparing their linear correlation coefficients, it was found that both Langmuir and Freundlich models could describe the adsorption behaviors of As(III) ions on the adsorbents, though the linear correlation coefficients for Freundlich model is slightly better (Table 2). This observation implies that monolayer adsorption as well as heterogeneous surface conditions may co-exist under the experimental conditions.

Table 1
Thermodynamic parameters for adsorption of As(III) ions on HS modified with $FeCl_3$ and $FeCl_3$ + NaOH

Adsorbent	ΔG° (kJ mol^{-1}) (at 20°C)	Δ*H*° (kJ mol^{-1})	Δ*S*° (kJ mol^{-1} K^{-1})
HS modified with $FeCl_3$	–2.31	–14.27	–0.0408
HS modified with $FeCl_3$ + NaOH	–5.52	–19.65	–0.0482

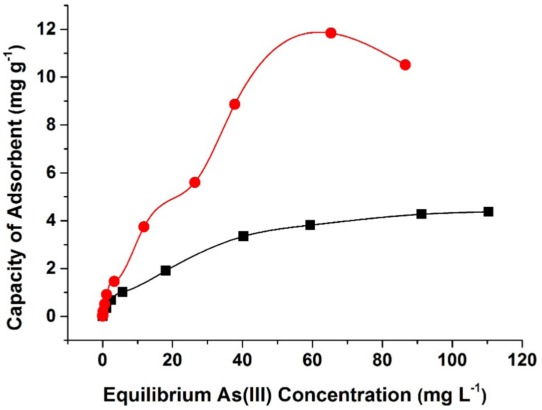

Fig. 6. Plots of q_e vs. equilibrium concentration of As(III): contact time for HS modified with $FeCl_3$ and HS modified with $FeCl_3$ + NaOH – 4 and 2 h, respectively; optimum pH – 9.0 ± 0.2; optimum temperature – 20°C; initial concentration – 0.05 mg L^{-1} and 0.1 g adsorbent (■: HS modified with $FeCl_3$; ●: HS modified with $FeCl_3$ + NaOH).

Table 2
Adsorption isotherm parameters for the adsorption of As(III) on the modified sorbents

Sorbents	Langmuir			Freundlich			
	q_m (mg g^{-1})	b (L mg^{-1})	R^2	K_f (mg g^{-1})	n	R^2	
HS modified with $FeCl_3$	4.85	0.0676	0.9776	0.257	1.48	0.9828	
HS modified with $FeCl_3$ + NaOH	12.56	0.0642	0.9074	0.633	1.42	0.9872	
	Temkin			Dubinin–Raduskevich			
	b_T (J mg^{-1})	A (g L^{-1})	R^2	q_m (mg g^{-1})	K (mol^2 kJ^{-2})	E (kJ mol^{-1})	R^2
HS modified with $FeCl_3$	4,643.26	8.57	0.8058	1.42	0.0523	3.092	0.7499
HS modified with $FeCl_3$ + NaOH	2,108.35	15.51	0.7172	2.99	0.0412	3.484	0.7871

3.5. Characterization of adsorbents

Fig. 7 shows scanning electron microscopy micrographs of bare HS, modified HS and also As(III) loaded modified HS. The surface change in the scanning electron microscopy micrographs indicated the structural changes in the adsorbent before and after arsenic treatment. The general morphology of the adsorbents before adsorption could be characterized as rough and irregular. The surfaces of the arsenic loaded HS modified with $FeCl_3$ and $FeCl_3$ + NaOH were noted to have much asperity. After adsorption, As(III) might be diffused into the porous structure.

EDX detector was used for structural analysis. It is given percentage of elements of adsorbents after As(III) adsorption and bare HS in Table 3. It can be calculated adsorbent capacities approximately using mass percentages of arsenic (0.41% and 1.26%) obtained from structural analysis. Capacities for HS modified with $FeCl_3$ and $FeCl_3$ + NaOH were 4.1 and 12.6 mg g^{-1}, respectively.

The various physico-chemical characteristics of the modified HSs are given in Table 4 according to the BET results. Surface area of HS modified with $FeCl_3$ is higher than the modified with $FeCl_3$ + NaOH. HS modified with $FeCl_3$ + NaOH

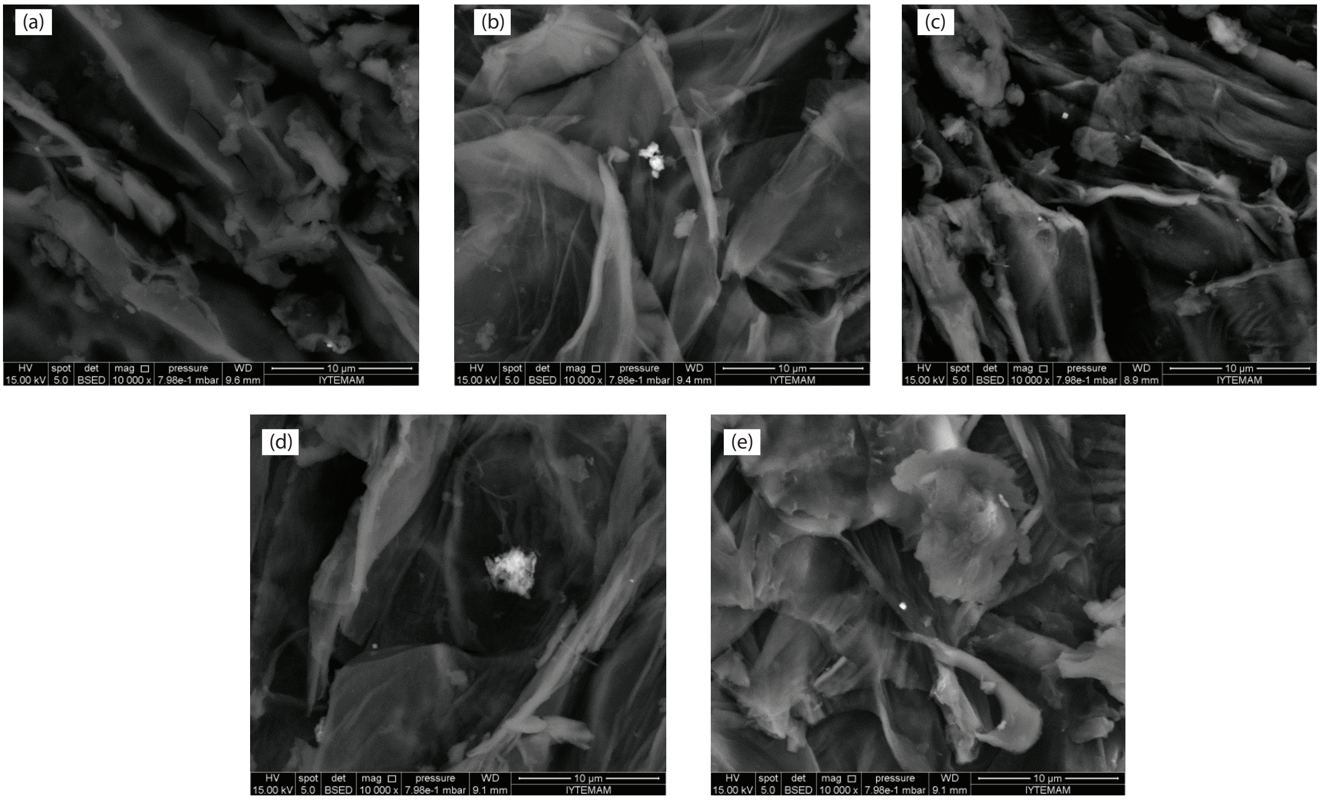

Fig. 7. Scanning electron microscopy micrographs of: (a) HS, (b) HS modified with $FeCl_3$, (c) As(III) loaded HS modified with $FeCl_3$, (d) HS modified with $FeCl_3$ + NaOH and (e) As(III) loaded HS modified with $FeCl_3$ + NaOH.

Table 3
Chemical composition of bare HS and modified adsorbents after arsenic adsorption

Element	Bare HS		HS modified with $FeCl_3$		HS modified with $FeCl_3$ + NaOH	
	Wt%	Atomic %	Wt%	Atomic %	Wt%	Atomic %
C	59.99	66.64	52.81	61.11	45.85	54.39
N	0.45	0.43	–	–	5.60	5.71
O	39.42	32.87	43.01	37.36	42.91	38.18
Na	–		0.80	0.49	–	–
S	0.14	0.06	0.13	0.05	–	–
Cl	–	–	1.46	0.57	2.30	0.94
Fe	–	–	1.38	0.34	2.08	0.54
As	–	–	0.41	0.08	1.26	0.24
Total	100.00	100.00	100.00	100.00	100.00	100.00

has higher capacity because of active group formation with different amounts. Similar results were obtained by Gülbaş et al. [29].

ATR–FTIR spectra of adsorbents are shown in Figs. 8 and 9. Spectral changes of HS + $FeCl_3$ and HS + $FeCl_3$ + NaOH modifications are demonstrated separately. Similar changes were observed for both modifications. The band around 1,028 cm^{-1} in bare HS associated with C–O stretching of alcoholic groups (OH) shifted after modification and shifted again with saturation. This may indicate that alcoholic groups could participate in modification and adsorption. There is no change among alcoholic O–H bands (3,300 cm^{-1}) because of low modification ratio (approximately 1%–2% Fe).

XRD patterns of the adsorbents shown in Fig. 10 demonstrate more amorphous phases that were formed by the dominating HS in both of them. Two diffraction peaks at $2\theta = 21.81°$ and 34.73° were clearly identified in both adsorbents. These peaks fit to goethite (FeOOH) with reference code 98-015-9957 according to High Score database.

For the determination of PZC, 0.01 M NaCl solutions were adjusted to pH = 3–9 using NaOH or HCl. Then 10 mL of solutions at different pH were taken in centrifuge tubes with 30 mg of adsorbent. These tubes were shaking for 24 h with mechanical shaker, and the initial and supernatant pH of the solutions were measured. The ΔpH was plotted against initial pH values, and the initial pH at which ΔpH was zero was considered as PZC (Fig. 11). PZC of HS + $FeCl_3$ and HS + $FeCl_3$ + NaOH values were determined as 4.0 and 4.2, respectively.

Images of bare HS and modified adsorbents are given in Fig. 12. The modification has also seen changes in the appearance of the adsorbents. An organo-metallic bond could be caused discoloration of sorbent (R–O–Fe). Adsorption mechanism occurring on modified adsorbents surfaces is most probably as coordination of hydroxyl groups of ferrous

Table 4
Physical characteristics of HS modified with $FeCl_3$ and $FeCl_3$ + NaOH

Physical characteristics	HS modified with $FeCl_3$	HS modified with $FeCl_3$ + NaOH
Single point surface area at $p°/p$	2.46 $m^2\ g^{-1}$	0.69 $m^2\ g^{-1}$
BET surface area	2.69 $m^2\ g^{-1}$	0.62 $m^2\ g^{-1}$
BJH adsorption cumulative surface area of pores between 17,000 and 3,000,000 Å width	0.91 $m^2\ g^{-1}$	3.08 $m^2\ g^{-1}$
BJH desorption cumulative surface area of pores between 17,000 and 3,000,000 Å width	0.75 $m^2\ g^{-1}$	–

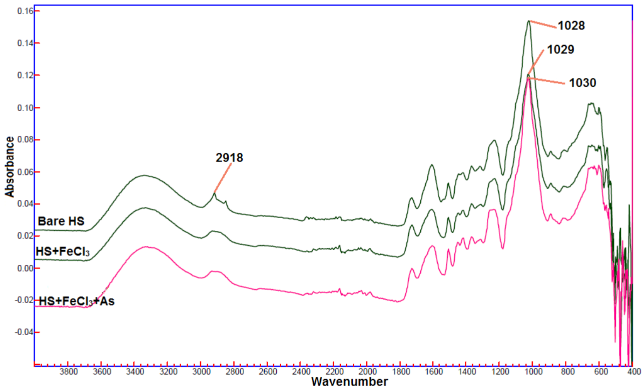

Fig. 8. ATR–FTIR spectra for: bare HS, HS + $FeCl_3$ and HS + $FeCl_3$ saturated with As(III).

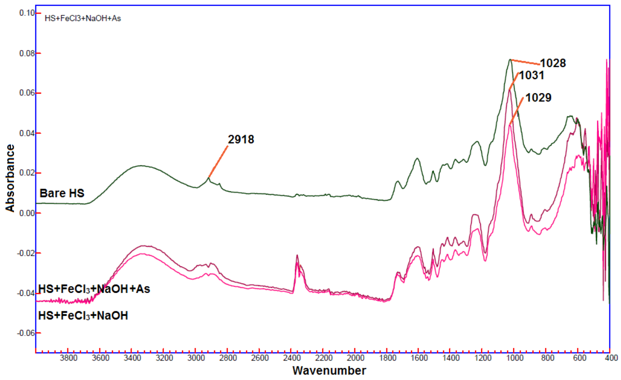

Fig. 9. ATR–FTIR spectra for: bare HS, HS + $FeCl_3$ + NaOH and HS + $FeCl_3$ + NaOH saturated with As(III).

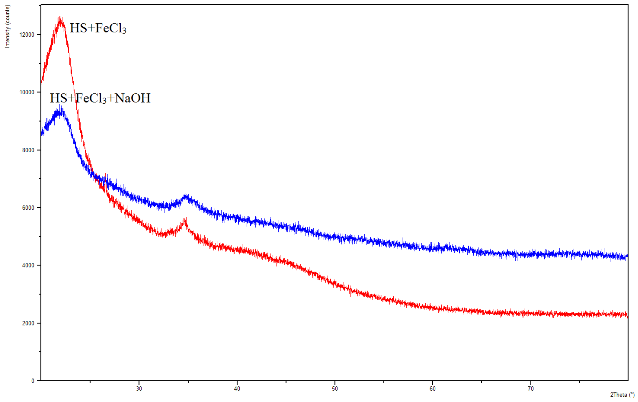

Fig. 10. XRD patterns of HS + $FeCl_3$ and HS + $FeCl_3$ + NaOH.

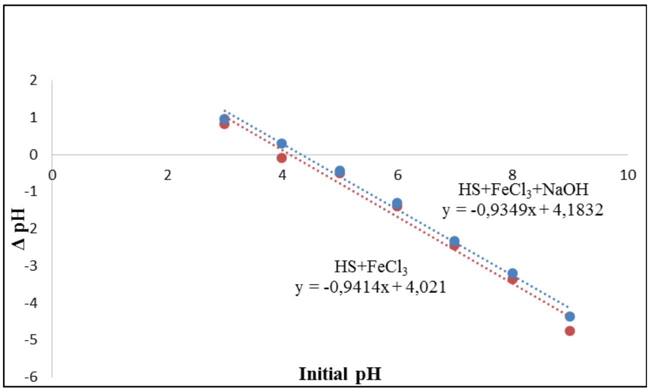

Fig. 11. Determination of PZC of adsorbents as function of ΔpH and initial pH.

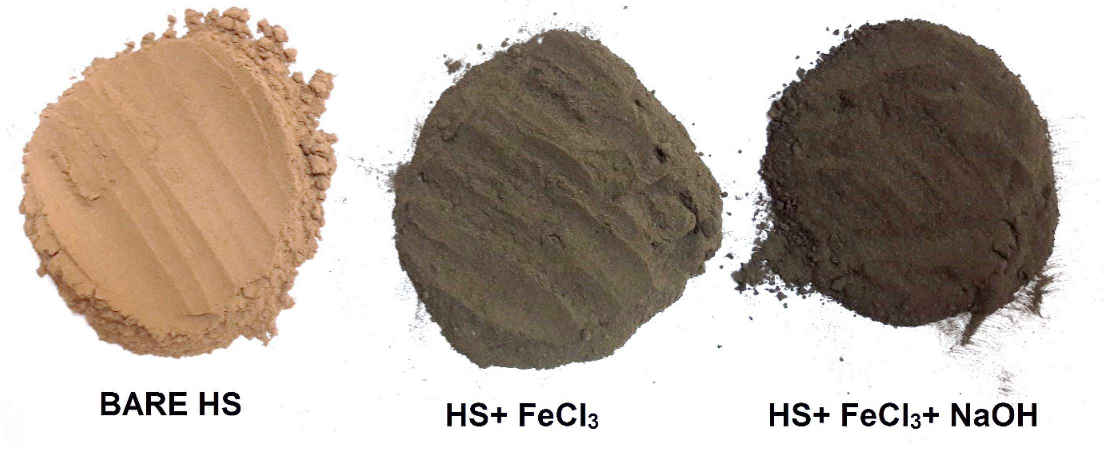

Fig. 12. Bare and modified adsorbents.

hydro(oxides) with the OH– ligands in the arsenite molecule (Fe–O–As). Similar mechanism was reported by Arcibar-Orozco et al. [31].

4. Conclusion

In the course of presented research, HS modified with $FeCl_3$ and $FeCl_3$ + NaOH were prepared as natural adsorbents to remove As(III) ions from aqueous solution. According to the batch studies pH = 9.0 ± 0.2 showed to have the highest adsorption for As(III) ions on both adsorbents, similar results were reported by Yadanaparthi et al. [32].

The adsorption process was exothermic ($\Delta H°$ ads < 0) and proceeds spontaneously ($\Delta G°$ ads < 0) for both adsorbents. Although surface area of HS modified with $FeCl_3$ is higher than the HS modified with $FeCl_3$ + NaOH, HS modified with $FeCl_3$ + NaOH has higher capacity. Because according to SEM–EDX analysis results, in the case of using NaOH for adsorbent modification, more iron ions hold on the adsorbent, and this could increase adsorption efficiency.

In this study adsorbents were treated with more concentrated solution of arsenic until adsorbents reach the saturation so that maximum capacity values determined for both adsorbents. Maximum adsorption experimental capacities of HS + $FeCl_3$ and HS + $FeCl_3$ + NaOH were 4.37 and 11.84 mg g^{-1} for arsenic, respectively. Capacities of some other natural sorbents were reported as Fe loaded sponge 18.0 mg g^{-1} [32], iron oxide coated biomass 0.880 mg g^{-1} [32], blast furnace slag 1.40 mg g^{-1} [33] and magnetite/non-oxidative graphene composites 38 mg g^{-1} [34]. Although performance of adsorbents at this study are not as high as carbonaceous materials or nanoparticles, they are considerably effective compared with other natural adsorbents. HS is common, and waste material became effective adsorbents with simple modifications. Manufacturing of these adsorbents is easy, and only the iron salt is required. Both adsorbents can be used to remove As(III) from water without pre-oxidation, and they provide low-cost alternatives for arsenic removal.

Acknowledgment

This study was supported by Celal Bayar University Research Foundation Project No: 2012-088.

Symbols

%A — Percentage adsorption of arsenic
C_{int} — Initial arsenic concentration, mg L^{-1}
C_{fin} — Final arsenic concentration, mg L^{-1}
q_e — Amount of arsenic ions adsorbed by adsorbent, mg g^{-1}
m — Mass of adsorbent, g
V — Volume of arsenic solution, mg g^{-1}
K_d — Distribution coefficient
C_e — Equilibrium arsenic concentration, mg L^{-1}
$\Delta G°$ — Free energy change, kJ mol^{-1}
$\Delta H°$ — Enthalpy change, kJ mol^{-1}
$\Delta S°$ — Entropy change, kJ mol^{-1} K^{-1}
R — Universal gas constant, 8.314 J mol^{-1} K^{-1}
T — Absolute temperature, K
q_e — Equilibrium adsorption capacity of adsorbent, mg g^{-1}
b — Langmuir adsorption constant, L mg^{-1}
q_m — Maximum amount of arsenic adsorbed, mg g^{-1}
K_f — Freundlich adsorption constant, mg g^{-1}
n — Freundlich adsorption constants
A — Temkin isotherm constant, L g^{-1}
b_T — Heat of adsorption, J mg^{-1}
ε — Polanyi potential, J mol^{-1}

References

[1] H.T. Fan, T. Sun, H.B. Xu, Y.J. Yang, Q. Tang, Y. Sun, Removal of arsenic(V) from aqueous solutions using 3-[2-(2-aminoethylamino) ethylamino]propyl-trimethoxysilane functionalized silica gel adsorbent, Desalination, 278 (2011) 238–243.

[2] Z. Li, J.S. Jean, W.T. Jiang, P.H. Chang, C.J. Chen, L. Liao, Removal of arsenic from water using Fe-exchanged natural zeolite, J. Hazard. Mater., 187 (2011) 318–323.

[3] P.K. Raul, R.R. Devi, I.M. Umlong, A.J. Thakur, S. Banerjee, V. Veer, Iron oxide hydroxide nanoflower assisted removal of arsenic from water, Mater. Res. Bull., 49 (2014) 360–368.

[4] T.S. Anirudhan, S. Jalajamony, Cellulose-based anion exchanger with tertiary amine functionality for the extraction of arsenic(V) from aqueous media, J. Environ. Manage., 91 (2010) 2201–2207.

[5] S. Mandal, T. Padhi, R.K. Patel, Studies on the removal of arsenic(III) from water by a novel hybrid material, J. Hazard. Mater., 192 (2011) 899–908.

[6] P. Chutia, S. Kato, T. Kojima, S. Satokawa, Arsenic adsorption from aqueous solution on synthetic zeolites, J. Hazard. Mater., 162 (2009) 440–447.

[7] D.D. Gang, B. Deng, L.S. Lin, As(III) removal using an iron-impregnated chitosan sorbent, J. Hazard. Mater., 182 (2010) 156–161.

[8] J.S Yamani, S.M. Miller, M.L. Spaulding, J.B. Zimmerman, Enhanced arsenic removal using mixed metal oxide impregnated chitosan beads, Water Res., 46 (2012) 4427–4434.

[9] G. Zhang, Z. Ren, X. Zhang, J. Chen, Nanostructured iron(III)-copper(II) binary oxide: a novel adsorbent for enhanced arsenic removal from aqueous solutions, Water Res., 47 (2013) 4022–4031.

[10] Y. Chammui, P. Sooksamiti, W. Naksataa, S. Thiansemc, O. Arqueropanyoa, Removal of arsenic from aqueous solution by adsorption on Leonardite, Chem. Eng. J., 240 (2014) 202–210.

[11] G. Pershagen, The carcinogenicity of arsenic, Environ. Health Perspect., 40 (1981) 93–100.

[12] A.H. Smith, C. Hopenhayn, M.N. Bates, H.M. Geoden, I. Hertapicciotto, H.M. Duggan, R. Wood, M.J. Kosnett, M.T. Smith, Cancer risks from arsenic in drinking water, Environ. Health Perspect., 97 (1992) 259–267.

[13] T.S.Y. Choong, T.G. Chuah, Y. Robiah, F.L.G. Koay, I. Azni, Arsenic toxicity, Health hazards and removal techniques from water: an overview, Desalination, 217 (2007) 139–166.

[14] Y. Glocheux, M.M. Pasarin, A.B. Albadarin, S.J. Allen, G.M. Walker, Removal of arsenic from groundwater by adsorption onto an acidified laterite by-product, Chem. Eng. J., 228 (2013) 565–574.

[15] R. Chen, Z. Lei, S. Yang, Z. Zhang, Y. Yang, N. Sugiura, Characterization and modification of porous ceramic sorbent for arsenate removal, Colloids Surf., A, 414 (2012) 393–399.

[16] M. Aryal, M. Ziagova, M. Liakopoulou-Kyriakides, Study on arsenic biosorption using Fe(III)-treated biomass of *Staphylococcus xylosus*, Chem. Eng. J., 162 (2010) 178–185.

[17] X. Guan, J. Du, X. Meng, Y. Sun, B. Sun, Q. Hu, Application of titanium dioxide in arsenic removal from water: a review, J. Hazard. Mater., 215–216 (2012) 1–16.

[18] S.A. Ntim, S. Mitra, Adsorption of arsenic on multiwall carbon nanotube–zirconia nanohybrid for potential drinking water purification, J. Colloid Interface Sci., 375 (2012) 154–159.

[19] K.N. Ghimire, K. Inoue, K. Makino, T. Miyajima, Adsorption removal of arsenic using orange juice residue, Sep. Sci. Technol., 37 (2002) 2785–2799.

[20] T.S. Anirudhan, M.R. Unnithan, Arsenic(V) removal from aqueous solutions using an anion exchanger derived from coconut coir pith and its recovery, Chemosphere, 66 (2007) 60–66.

[21] M.N. Amin, S. Kaneco, T. Kitagawa, A. Begum, H. Katsumata, T. Suzuki, K. Ohta, Removal of arsenic in aqueous solutions by adsorption onto waste rice husk, Ind. Eng. Chem. Res., 45 (2006) 8105–8110.

[22] I.A. Oke, N.O. Olarinoye, S.R.A. Adewusi, Adsorption kinetics for arsenic removal from aqueous solutions by untreated powdered eggshell, Adsorption, 14 (2008) 73–83.

[23] M.C. Teixeira, V.S.T. Ciminelli, Development of a biosorbent for arsenite: structural modeling based on X-ray spectroscopy, Environ. Sci. Technol., 39 (2005) 895–900.

[24] Ş. Targan, V.N. Tirtom, Arsenic removal from aqueous system using modified chestnut shell, Desal. Wat. Treat., 56 (2015) 1029–1036.

[25] R.C. Vaishya, S.K. Gupta, Modeling arsenic(V) removal from water by sulfate modified iron-oxide coated sand (SMIOCS), J. Chem. Technol. Biotechnol., 78 (2002) 73–80.

[26] J. Hlavay, K. Polyak, Determination of surface properties of iron hydroxidecoated alumina adsorbent prepared for removal of arsenic from drinking water, J. Colloid Interface Sci., 284 (2005) 71–77.

[27] F.S. Zhang, H. Itoh, Iron oxide-loaded slag for arsenic removal from aqueous system, Chemosphere, 60 (2005) 319–325.

[28] H. Matsunaga, T. Yokoyama, R.J. Eldridge, B.A. Bolto, Adsorption characteristics of arsenic(III) and arsenic(V) on iron(III)-loaded chelating resin having lysine-N^{α},N^{α}-diacetic acid moiety, React. Funct. Polym., 29 (1996) 167–174.

[29] G. Gülbaş, V.N. Tirtom, A. Çelik, K. Dost, Arsenic removal from aqueous system using natural and modified (kula ebonite and zeolite) adsorbents, Environ. Prog. Sustain. Energy, 31 (2011) 443–448.

[30] M. Kosmulski, Isoelectric points and points of zero charge of metal (hydr)oxides: 50 years after Parks' review, Adv. Colloid Interface Sci., 238 (2016) 1–61.

[31] J.A. Arcibar-Orozco, D. Josue, J.C. Rios-Hurtado, J.R. Rangel-Mendez, Influence of iron content, surface area and charge distribution in the arsenic removal by activated carbons, Chem. Eng. J., 249 (2014) 201–209.

[32] S.K.R. Yadanaparthi, D. Graybill, R. Wandruszka, Adsorbents for the removal of arsenic, cadmium, and lead from contaminated waters, J. Hazard. Mater., 171 (2009) 1–15.

[33] S.R. Kanel, H. Choi, J.-Y. Kim, S. Vigneswaran, W.G. Shim, Removal of arsenic(III) from groundwater using low-cost industrial by-products-blast furnace slag, Water Qual. Res. J. Can., 41 (2006) 130–139.

[34] Y. Yoon, M. Zheng, Y. Ahn, W.K. Park, W.S. Yang, J. Kang, Synthesis of magnetite/non-oxidative graphene composites and their application for arsenic removal, Sep. Purif. Technol., 178 (2017) 40–48.